Int. J. Heat Mass Transfer. Vol. 35, No. 4, pp. 815–822, 1992
Printed in Great Britain

0017–9310/92 $5.00 + 0.00
Pergamon Press plc

Analysis of conjugate laminar mixed convection cooling in a shrouded array of electronic components

SUBHASHIS RAY and J. SRINIVASAN
Department of Mechanical Engineering, Indian Institute of Science, Bangalore 560012, India

(*Received* 17 *July* 1989 *and in final form* 14 *January* 1991)

Abstract—The temperature variation in the insulation around an electronic component, mounted on a horizontal circuit board is studied numerically. The flow is assumed to be laminar and fully developed. The effect of mixed convection and two different types of insulation are considered. The mass, momentum and energy conservation equations in the fluid and conduction equation in the insulation are solved using the SIMPLER algorithm. Computations are carried out for liquid Freon and water, for different conductivity ratios, and different Rayleigh numbers. It is demonstrated that the temperature variation within the insulation becomes important when the thermal conductivity of the insulation is less than ten times the thermal conductivity of the cooling medium.

INTRODUCTION

COOLING of electronic equipment has been studied in great detail in recent years. When the heat dissipation from the electronic equipment is higher than 0.1 W cm^{-2}, immersion forced convection cooling by liquids, such as Freon and water, is used. When the electronic circuit boards are stacked horizontally, we obtain a combination of shrouds and rectangular heat sources as shown in Fig. 1. Braaten and Patankar [1] presented a study of laminar mixed convection for the geometry shown in Fig. 1. They modelled the electronic components as a uniform heat generating block with infinite thermal conductivity. They also assumed the flow to be hydrodynamically and thermally fully developed. This assumption is valid when the gap between the components in the axial direction is small. They have demonstrated that buoyancy can enhance heat transfer significantly. The model proposed by Braaten and Patankar [1] for the electronic components is reasonable if a fluid like air is used as a cooling medium. If fluids like Freon or water are used as cooling media then the temperature variation within the insulation, surrounding the chip, can be comparable to that between the wall of the package and the fluid. Hence, it is necessary to account for the temperature variation within the insulation to predict the chip temperature. The thermal conductivities of the chip, the leads and the heat spreaders are large compared to that of the insulation and hence, they can be assumed to be at constant temperature. In this paper we have extended the work of Braaten and Patankar [1] to account for the temperature variation within the insulation.

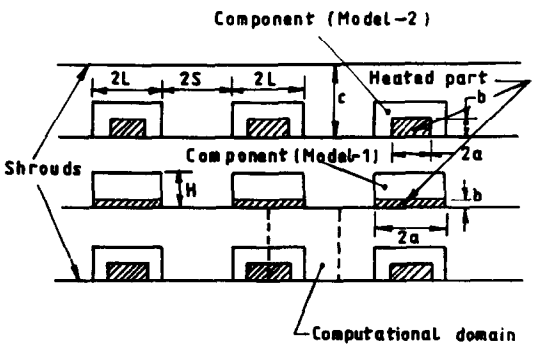

FIG. 1. Geometry of present work.

PRESENT MODEL AND PROBLEM FORMULATION

We are aware of only two papers [2, 3] where the investigators have modelled the chip and the insulations separately. They have assumed the chip to be covered by the insulation from all sides. This assumption is valid for surface-mounted components, but not for dual in-line processors. The leads and heat spreaders for dual in-line processors are exposed to the cooling fluid and allow the convective cooling to occur from the sides. We have considered two possible configurations. One, in which the insulation is present only on the top of the chip and the other, in which the insulation is present both on the top and sides (Fig. 2). We have assumed the bottom of the chip to be perfectly insulated. We have assumed the flow to be hydrodynamically and thermally fully developed in the axial direction as assumed by Braaten and Patankar [1]. Our primary objective is the prediction of the chip temperature. We have already observed in Fig. 1 that, due to the symmetry of this problem, we

NOMENCLATURE

a, A	dimensional and dimensionless half width of the heat generating part
A_b	surface area of the block per unit axial length of the computational module, $H+L$
A_c	cross-sectional area of the computational domain open to flow, $C[L+S]-HL$
b, B	dimensional and dimensionless height of the heat generating part
C	spacing between shrouds
C_p	specific heat at constant pressure
g	acceleration due to gravity
h, H	dimensional and dimensionless height of the block
h_c	average heat transfer coefficient
k_f	thermal conductivity of the fluid
k_s	thermal conductivity of the solid
K_r	conductivity ratio, k_s/k_f
l, L	dimensional and dimensionless half width of the block
Nu	average Nusselt number, $h_c H/k_f$
p	pressure
$\bar{p}$	mean pressure averaged over the passage cross-section
p^*	effective pressure, $p+\rho_c gy$
P	dimensionless pressure
Pr	Prandtl number, ν/α
$\dot{Q}'$	heat dissipation per unit axial length of the computational module
Ra	Rayleigh number
s, S	dimensional and dimensionless half spacing between the blocks
T	temperature
$T_b, \bar{T}_w$	bulk fluid temperature, average wall temperature of the block
u, U, v, V, w, W	dimensional and dimensionless velocity components in the x-, y-, z-directions
x, X, y, Y, z, Z	dimensional and dimensionless horizontal, vertical and axial coordinates.

Greek symbols

α	thermal diffusivity of the fluid
β	thermal expansion coefficient of the fluid
θ	dimensionless temperature
θ_b	dimensionless bulk temperature
$\bar{\theta}_w$	dimensionless average wall temperature
ν	kinematic viscosity of the fluid
ρ	fluid density
ρ_c	fluid density at temperature T_c
ψ	dimensionless stream function.

can find a typical repeating module (in the x–y plane) and hence, we have analysed that module only. We have solved the governing continuity, momentum and energy equations for a quasi-three-dimensional laminar flow for an incompressible Newtonian fluid. The Boussinesq approximation has been made to account for the free convection effects. We express the buoyancy term, ρg, as

$$\rho g = \rho_c[1-\beta(T-T_c)]g$$
$$= \rho_c g - \rho_c\beta(T-T_c)g.$$

The term $\rho_c g$ is absorbed in the pressure term by defining an effective pressure

$$p^* = p+\rho_c gy.$$

As the flow is hydrodynamically fully developed, all the velocity gradients in the axial direction vanish ($\partial u/\partial z = \partial v/\partial z = \partial w/\partial z = 0$). The axial pressure gradient is replaced by $\partial\bar{p}/\partial z$, where $\bar{p}$ is the mean pressure averaged over the cross-section of the passage. $\partial\bar{p}/\partial z$ is taken as constant. For fully developed laminar flow with a boundary condition of

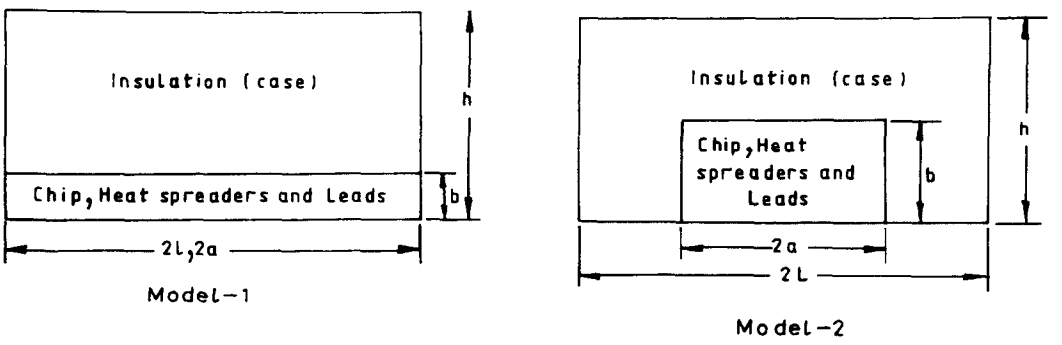

FIG. 2. Proposed models of the package.

uniform heat flux per unit axial length, all temperature rise will be linear with axial distance and hence, we obtain

$$\partial T/\partial z = \partial T_c/\partial z = \partial T_b/\partial z.$$

Again, from the energy balance, we obtain

$$dT_b/dz = \dot{Q}'/(\rho C_p \bar{w} A_c).$$

We have defined the following non-dimensional quantities in order to express the governing equations in the dimensionless form

$$X = x/C, \quad Y = y/C, \quad S = s/C, \quad L = l/C$$

$$H = h/C, \quad A = a/C, \quad B = b/C$$

$$U = uC/\alpha, \quad V = vC/\alpha, \quad W = \rho vw/(-d\bar{p}/dz)C^2$$

$$\theta = k_f(T - T_c)/\dot{Q}', \quad P = p^* C^2/(\rho\alpha^2)$$

$$Pr = \nu/\alpha, \quad Ra = g\beta\dot{Q}'C^3/(\alpha\nu k_f).$$

Substituting these dimensionless variables in the conservation equations, we obtain

$$\frac{\partial U}{\partial X} + \frac{\partial V}{\partial Y} = 0$$

$$U\frac{\partial U}{\partial X} + V\frac{\partial U}{\partial Y} = -\frac{\partial P}{\partial X} + Pr\left[\frac{\partial^2 U}{\partial X^2} + \frac{\partial^2 U}{\partial Y^2}\right]$$

$$U\frac{\partial V}{\partial X} + V\frac{\partial V}{\partial Y} = -\frac{\partial P}{\partial Y} + Ra\,Pr\,\theta + Pr\left[\frac{\partial^2 V}{\partial X^2} + \frac{\partial^2 V}{\partial Y^2}\right]$$

$$U\frac{\partial W}{\partial X} + V\frac{\partial W}{\partial Y} = Pr + Pr\left[\frac{\partial^2 W}{\partial X^2} + \frac{\partial^2 W}{\partial Y^2}\right]$$

$$U\frac{\partial \theta}{\partial X} + V\frac{\partial \theta}{\partial Y} = \left[\frac{\partial^2 \theta}{\partial X^2} + \frac{\partial^2 \theta}{\partial Y^2}\right] - \left[\frac{C^2}{A_c}\right]\frac{W}{\bar{W}}.$$

In addition to these, we have one more energy equation for the solid (insulation)

$$\left[\frac{\partial^2 \theta}{\partial X^2} + \frac{\partial^2 \theta}{\partial Y^2}\right] = 0.$$

Here, we have neglected the axial conduction within the insulation.

The coefficient C^2/A_c is only a function of geometric parameters (S, L, H). We have taken $S = 0.5$, $L = 0.5$, and $H = 0.5$ for the present analysis. We have taken $A = 0.5$ and $B = 0.1$ for model 1 and $A = 0.25$ and $B = 0.25$ for model 2. The geometric parameters are kept fixed for the problem.

The boundary conditions (shown in Fig. 3)

At $X = 0$, for all Y

$$U = 0, \quad \partial V/\partial X = 0, \quad \partial W/\partial X = 0,$$

$$\partial T/\partial X = \partial\theta/\partial X = 0.$$

At $X = L + S$, for all Y

$$U = 0, \quad \partial V/\partial X = 0, \quad \partial W/\partial X = 0,$$

$$\partial T/\partial X = \partial\theta/\partial X = 0.$$

At $Y = 0$, for all X

$$U = 0, \quad V = 0, \quad W = 0, \quad \partial T/\partial Y = \partial\theta/\partial Y = 0.$$

At $Y = C$, for all X

$$U = 0, \quad V = 0, \quad W = 0, \quad \partial T/\partial Y = \partial\theta/\partial Y = 0.$$

All the velocities within the solids are zero. $T = T_c$ or, $\theta = 0$ on the heat generating part. At the solid–liquid interface the fluxes are matched, for example, at $X = L, Y < H$

$$k_s \left.\frac{\partial T}{\partial X}\right|_{L^-} = k_f \left.\frac{\partial T}{\partial X}\right|_{L^+}$$

$$\text{or} \quad k_s \left.\frac{\partial \theta}{\partial X}\right|_{L^-} = k_f \left.\frac{\partial \theta}{\partial X}\right|_{L^+}.$$

This boundary condition at the interface is taken care of by employing an interface conductivity, as prescribed by Patankar [4].

We have discretized the conservation equations governing the flow and heat transfer in this problem by the control volume approach, as described in ref. [4]. The computations were carried out on a DEC-1090 system using the SIMPLER algorithm [4]. The ADI method is used to solve the discretized equations.

After obtaining the converged solutions, we have

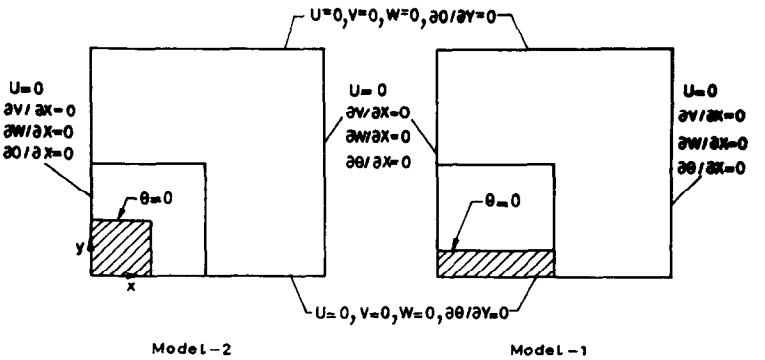

FIG. 3. Computational domain with conditions at the boundary (predominant flow is perpendicular to the figure).

calculated the non-dimensional stream-function. This is defined as

$$\partial\psi/\partial Y = U \quad \text{and} \quad \partial\psi/\partial X = -V.$$

We have also calculated the heat transfer coefficient and Nusselt number from the converged solutions. We have defined the average heat transfer coefficient (h_c) as

$$h_c = \dot{Q}'/[A_b(\bar{T}_w - T_b)].$$

Hence, the Nusselt number

$$Nu = h_c H/k_f$$
$$= \frac{\dot{Q}' H}{k_f[H+L][\bar{T}_w - T_c - (T_b - T_c)]}$$
$$= 1/[(1+L/H)(\bar{\theta}_w - \theta_b)].$$

We have chosen a 22×22 grid for our solution with a uniformly distributed grid over most of the domain and finer grids near the interface between the block and the fluid. We have checked the maximum of the mass residues over the control volumes after each iteration. The convergence criterion is varied from 10^{-3} to 10^{-6} for different Rayleigh numbers. At low Rayleigh numbers and high conductivity ratios, the converged solutions are obtained in a few hundred iterations. As the Rayleigh number increases, or the conductivity ratio decreases, the number of iterations required to achieve the converged solutions increase. We have reduced the convergence criterion further and calculated the Nusselt number and non-dimensional chip temperature (T_r, defined later) and checked the variations in their values. The final solution is obtained when these variations are less than 0.1%. We have increased the number of grids to 28×28 and obtained some of the solutions. We observed that the Nusselt number and the non-dimensional chip temperature vary only at the third decimal place.

The computer code was validated by calculating the Nu for different Ra, for Freon, with infinite conductivity ratio. The Nusselt number obtained was found to be within 1% of the solutions obtained by Braaten and Patankar [1].

RESULTS AND DISCUSSION

We have obtained the solutions for different Rayleigh numbers, ranging from 0 to 10^6 for fluids with $Pr = 3.5$, corresponding to liquid Freon and $Pr = 7.0$, corresponding to water for different conductivity ratios. For Freon as the coolant, we have chosen the conductivity ratio to be 5.0, 10.0 and 20.0. For water as the coolant, we have analysed the flow for $K_r = 2.0$ and 4.0. Note that the thermal conductivity of the insulation varies from 0.6 to 2.0 W m^{-1} K^{-1}, whereas, the thermal conductivities of liquid Freon and water are 0.075 and 0.6 W m^{-1} K^{-1}, respectively. We have only obtained the single eddy solution. We have also studied different cases for air, with $Pr = 0.7$. Since the thermal conductivity of air is very low, as compared to the thermal conductivity of insulation, we observed that the temperature variation within the insulation is not important and hence we have not presented any result for air as coolant.

Isotherms and streamlines

We consider first, the systems cooled by liquid Freon. The isotherms are presented for model 1 for $Ra = 10^6$ for $K_r = 5.0$ and 20.0 in Figs. 4(a) and (b). The values 0.1, 0.2, etc. are the values of $(\theta - \theta_{min})/(\theta_{max} - \theta_{min})$. In Figs. 5(a) and (b), we have presented the isotherms for model 2, for the same Rayleigh number and conductivity ratio. We observe that as the conductivity ratio decreases, there are more isotherms within the insulation—which indicates that the temperature variation within the insulation becomes more important for lower conductivity ratios. In Figs. 6(a) and (b), we have presented the isotherms for Freon cooled systems, for $Ra = 10^5$, $K_r = 5.0$ and 20.0 for model 1. We observe that as the Rayleigh number decreases (i.e. when the heat dissipated by the electronic component is less) then the effect of buoyancy on flow and heat transfer also becomes less and hence,

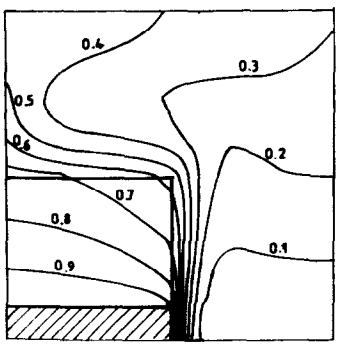

FIG. 4(a). Isotherms for $Pr = 3.5$, $Ra = 10^6$, $K_r = 5.0$, model 1.

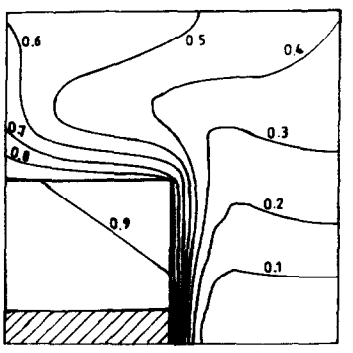

FIG. 4(b). Isotherms for $Pr = 3.5$, $Ra = 10^6$, $K_r = 20.0$, model 1.

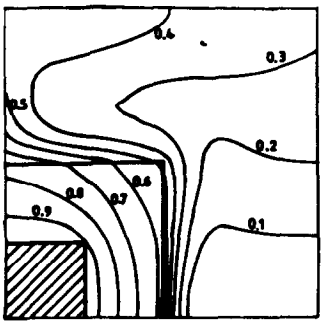

FIG. 5(a). Isotherms for $Pr = 3.5$, $Ra = 10^6$, $K_r = 5.0$, model 2.

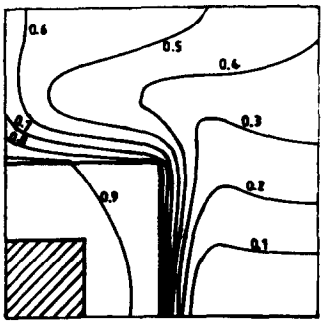

FIG. 5(b). Isotherms for $Pr = 3.5$, $Ra = 10^6$, $K_r = 20.0$, model 2.

the strength of secondary circulation is also less. Thus, for higher Rayleigh numbers, the secondary flow velocities are higher, which tend to shift the isotherms towards the left of the figure. We have presented the streamline plots for Freon as the cooling medium, for $K_r = 20.0$ and $Ra = 10^5$ and 10^6 in Figs. 7(a) and (b), respectively. The values 0.1, 0.2, etc. are the values of $(\psi - \psi_{min})/(\psi_{max} - \psi_{min})$.

Calculation of heat transfer coefficient and Nusselt number

We have not presented the variation of the Nusselt number as a function of Rayleigh number for the systems cooled with liquid Freon because the variation of the Nusselt number is within 2% of the solutions obtained by neglecting the temperature variation inside the insulation. We have presented the plot of the Nusselt number as a function of the Rayleigh number for the systems cooled by water, for $K_r = \infty$ in Fig. 8. We have observed that the variation of the Nusselt number for the conductivity ratio of 2.0 is within 5% of the solution obtained where the temperature variation within the insulation is neglected. We have also observed that there is hardly any change in the Nusselt number between models 1 and 2.

Non-dimensional chip temperature

The Nusselt number variation for different conductivity ratios and different Rayleigh numbers, alone, is not important for evaluating the maximum temperature attained by the chip. We have defined the non-dimensional chip temperature as

$$T_r = (T_c - \bar{T}_w)/(\bar{T}_w - T_b).$$

The non-dimensional chip temperature is the ratio of the temperature drop in the insulation to the temperature drop in the fluid. We have presented the variation of T_r to indicate the relative strength of the conduction within the insulation and the convection outside the package.

In Fig. 9(a), we have presented the variation of the non-dimensional chip temperature with Rayleigh number for different conductivity ratios for model 1. From the figure, we observe that T_r increases with the increase in Rayleigh number. Free convection is not playing any significant role in heat transfer below a Rayleigh number of 10^3 and hence, T_r remains constant up to a Rayleigh number of 10^3. The effect of temperature variation within the insulation becomes more important for higher Rayleigh numbers and lower conductivity ratios. In Fig. 9(b), we have pre-

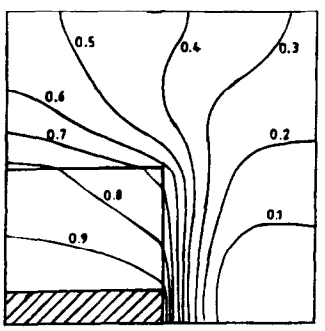

FIG. 6(a). Isotherms for $Pr = 3.5$, $Ra = 10^5$, $K_r = 5.0$, model 1.

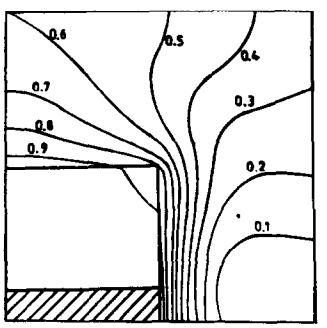

FIG. 6(b). Isotherms for $Pr = 3.5$, $Ra = 10^5$, $K_r = 20.0$, model 1.

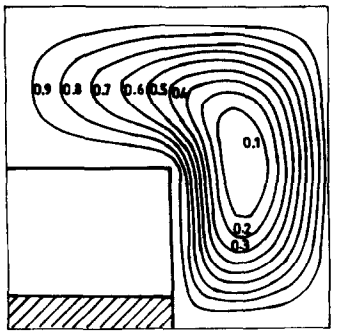

FIG. 7(a). Streamlines for $Pr = 3.5$, $Ra = 10^5$, $K_r = 20.0$, model 1.

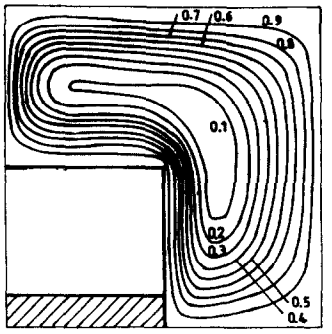

FIG. 7(b). Streamlines for $Pr = 3.5$, $Ra = 10^6$, $K_r = 20.0$, model 1.

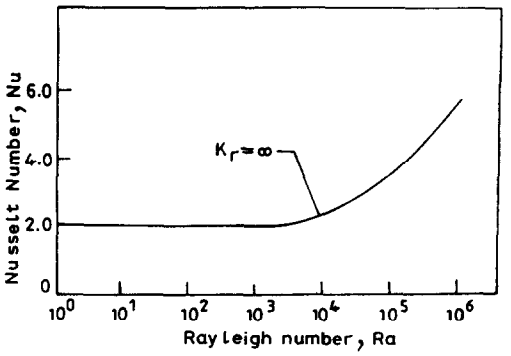

FIG. 8. *Nu* vs *Ra*, for water ($Pr = 7.0$), models 1 and 2.

sented the variation of T_r with Rayleigh number for model 2. These plots also show the similar trend as the previous one, but the values of T_r are higher than those obtained for model 1, for the same Rayleigh number and conductivity ratio. In model 1, we have assumed that the heat generating block is extended up to the boundary of the solid, whereas, in model 2, we have assumed that the heat generating block is covered by the insulation from all sides. The assumption of model 1 allows the fluid to come in contact with the heat generating part and hence, the fluid can take away the heat directly from this part. In the case of model 2, the heat generating part is not in direct contact with the fluid and hence the heat is transferred by conduction up to the wall of the solid block and from the wall it is taken away, by convection, by the fluid. This allows a lower value of $T_c - \bar{T}_w$ and hence, T_r for model 1 is also lower. Note, that for both the models $\bar{T}_w - T_b$ remains almost the same. Also note that, for a Rayleigh number of 10^6 and $K_r = 10.0$ the temperature drop in the insulation is about 50% of the temperature drop in the fluid. Hence, we can conclude that the conjugate problem must be considered for $K_r \leqslant 10.0$.

In Figs. 10(a) and (b) we have presented the variation of non-dimensional chip temperature with Rayleigh number for water cooled systems for models 1 and 2, respectively. The observations are similar to the previous cases, where Freon is used as the cooling medium.

Design calculations

So far we have discussed the effects of Rayleigh number and conductivity ratio on heat transfer for different cooling media. Although we have presented the variations of T_r with Rayleigh number for different K_r, different models and different coolants, we have not discussed the impact of these results on the prediction of the chip temperature.

Let us consider a case where water is used as the coolant. The spacing between the shrouds is 0.6 cm,

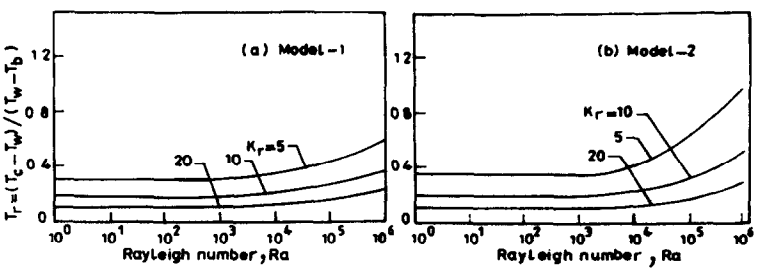

FIG. 9. Non-dimensional chip temperature vs Rayleigh number for $Pr = 3.5$.

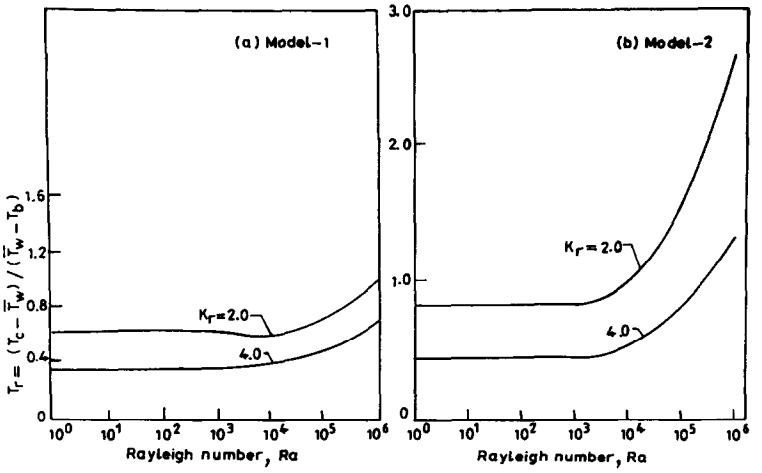

FIG. 10. Non-dimensional chip temperature vs Rayleigh number for $Pr = 7.0$.

and the heat dissipated by the components per unit axial length is 0.1 kW m^{-1}. This gives us a Rayleigh number of 8.5×10^6. Let us assume that the components are such that they can be simulated by model 1 and the conductivity ratio is 2.0. Now from Fig. 11, we can find out the value of $k_f(T_c - T_b)/\dot{Q}'$ as 0.165. This gives us

$$T_c - T_b = 27.5°C.$$

Now, if we neglect the temperature variation within the insulation and calculate the same, from the Nusselt number, then, we will obtain

$$T_c - T_b = 10.4°C.$$

Hence, the error in predicting the temperature difference between the chip and the bulk is 62%.

From simple energy balance, the bulk temperature of the fluid at any axial location can be calculated by knowing the inlet temperature of the fluid, heat dissipation rate, average axial velocity of the fluid, and the geometry. Hence, the chip temperature at any axial location can also be predicted with no difficulty.

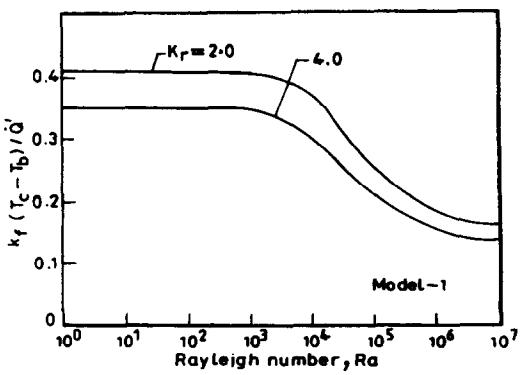

FIG. 11. $k_f(T_c - T_b)/\dot{Q}'$ vs Ra for $Pr = 7.0$.

Similar results have been presented by Ray [5] for water and Freon as coolant, for both the models.

CONCLUSIONS

The following conclusions can be drawn from our present study:

(1) The average Nusselt number, and hence the average heat transfer coefficient, is not a strong function of the conductivity ratio and the different models.

(2) The temperature variation within the insulation becomes more important in the case of a low conductivity ratio and a high Rayleigh number. There can be substantial error in predicting the chip temperature if the temperature variation within the insulation is neglected.

(3) The conjugate problem has to be considered for $K_r \leqslant 10.0$.

Acknowledgement—We are thankful to Dr R. L. Mahajan, from AT&T and Bell Laboratories, Princeton, for his valuable advice and suggestions during the course of this project.

REFERENCES

1. M. E. Braaten and S. V. Patankar, Analysis of laminar mixed convection in shrouded arrays of heated rectangular blocks, *Int. J. Heat Mass Transfer* **28**, 1699–1709 (1985).
2. A. Zebib and Y. K. Wo, A two-dimensional conjugate heat transfer model for forced air cooling of an electronic device, *Trans. ASME J. Electronic Packaging* **111**, 41–45 (1989).
3. Y. Asako and M. Faghri, Three-dimensional heat transfer analysis of arrays of heated square blocks, *Int. J. Heat Mass Transfer* **32**, 395–405 (1989).
4. S. V. Patankar, *Numerical Heat Transfer and Fluid Flow*. Hemisphere, New York (1980).
5. S. Ray, Analysis of conjugate laminar mixed convection in shrouded arrays of heated rectangular blocks, M.E. Thesis, Indian Institute of Science, Bangalore, India (1989).

ANALYSE DU REFROIDISSEMENT D'UN ARRANGEMENT DE COMPOSANTS ELECTRONIQUES PAR CONVECTION LAMINAIRE MIXTE, CONJUGUEE

Résumé—On étudie numériquement la variation de température dans l'isolant autour d'un composant électronique monté sur un tableau horizontal. L'écoulement est supposé laminaire et pleinement établi. On considère l'effet de la convection mixte et deux types différents d'isolation. Les équations de bilan de masse, quantité de mouvement et d'énergie dans le fluide et l'équation de conduction dans l'isolant sont résolues par algorithme SIMPLER. Les calculs sont faits pour le Freon et l'eau liquide, pour différents rapports de conductivité et différents nombres de Rayleigh. On montre que la variation de température dans l'isolant devient importante quand la conductivité de l'isolant est au moins dix fois la conductivité thermique du milieu refroidissant.

UNTERSUCHUNG DER KÜHLUNG DURCH KONJUGIERTE MISCHKONVEKTION IN EINER GEKAPSELTEN ANORDNUNG ELEKTRONISCHER BAUTEILE

Zusammenfassung—Die Temperaturverteilung der Isolation eines auf eine waagerechte Platine montierten elektronischen Bauteils wird numerisch untersucht. Dabei wird die Strömung als laminar und voll ausgebildet betrachtet. Es wird der Einfluß der Mischkonvektion und zweier unterschiedlicher Isolationsarten berücksichtigt. Die Massen-, Impuls- und Energie-Erhaltungssätze im Fluid sowie die Wärmeleitungsgleichung in der Isolation werden mit Hilfe des SIMPLER-Verfahrens gelöst. Berechnungen werden für Kältemittel und Wasser, für verschiedene Verhältnisse der Wärmeleitfähigkeiten und verschiedene Rayleigh-Zahlen durchgeführt. Es wird veranschaulicht, daß die Temperaturverteilung in der Isolation dann wichtig wird, wenn die Wärmeleitfähigkeit der Isolation weniger als das Zehnfache der Wärmeleitfähigkeit des Kühlmediums beträgt.

АНАЛИЗ СОПРЯЖЕННОЙ ЗАДАЧИ ОХЛАЖДЕНИЯ ЗА СЧЕТ ЛАМИНАРНОЙ СМЕШАННОЙ КОВЕКЦИИ ПРИ ЭКРАНИРОВАНИИ ЭЛЕКТРОННЫХ ЭЛЕМЕНТОВ

Аннотация—Численно исследуется изменение температур в изоляционном слое электронного элемента. Предполагается, что течение является ламинарным и полностью развитым. Рассматриваются случай смешанной конвекции и два различных типа изоляционного материала. С использованием алгоритма SIMPLER решаются уравнения сохранения массы, количества движения и энергии в жидкости, а также уравнение теплопроводности в изоляционном материале. Проводятся расчеты для жидкого хладагента и воды при различных отношениях теплопроводности и разных числах Рейнольдса. Показано, что изменение температур в изоляционном слое является существенным, когда его теплопроводность становится ниже теплопроводности охлаждающей среды в 10 раз.